arXiv:1512.07615v1 [physics.med-ph] 23 Dec 2015

Modeling of Radiation Pneumonitis after Lung Stereotactic Body Radiotherapy: A Bayesian Network Approach

Sangkyu Lee[a], Norma Ybarra[a], Krishinima Jeyaseelan[a], Sergio Faria[b], Neil Kopek[b], Pascale Brisebois[b], Toni Vu[c], Edith Filion[c], Marie-Pierre Campeau[c], Louise Lambert[c], Pierre Del Vecchio[c], Diane Trudel[c], Nidale El-Sokhn[c], Michael Roach[d], Clifford Robinson[d], Issam El Naqa[a,e]

[a] *Medical Physics Unit, McGill University, Montreal, Canada*
[b] *Department of Radiation Oncology, Cedars Cancer Centre, Montreal, Canada*
[c] *Department of Radiation Oncology, Centre Hospitalier de l'Université de Montréal, Montreal, Canada*
[d] *Department of Radiation Oncology, Washington University in St. Louis, St. Louis, United States*
[e] *Department of Radiation Oncology, University of Michigan, Ann Arbor, United States*

Abstract

Background and Purpose: Stereotactic body radiotherapy (SBRT) for lung cancer accompanies a non-negligible risk of radiation pneumonitis (RP). This study presents a Bayesian network (BN) model that connects biological, dosimetric, and clinical RP risk factors.

Material and Methods: 43 non-small-cell lung cancer patients treated with SBRT with 5 fractions or less were studied. Candidate RP risk factors included dose-volume parameters, previously reported clinical RP factors, 6 protein biomarkers at baseline and 6 weeks post-treatment. A BN ensemble model was built from a subset of the variables in a training cohort (N=32), and further tested in an independent validation cohort (N=11).

Results: Key factors identified in the BN ensemble for predicting RP risk were ipsilateral V5, lung volume receiving more than 105% of prescription, and decrease in angiotensin converting enzyme (ACE) from baseline to 6 weeks. External validation of the BN ensemble model yielded an area under the curve of 0.8.

Conclusions: The BN model identified potential key players in SBRT-induced RP such as high dose spillage in lung and changes in ACE expression levels. Predictive potential of the model is promising due to its probabilistic characteristics.

Keywords: radiation pneumonitis, stereotactic body radiotherapy, biomarkers, ensemble method, Bayesian network

1. Introduction

In recent years, stereotactic body radiotherapy (SBRT) has become the treatment of choice for non-operable early stage non-small cell lung cancer (NSCLC), demonstrating a local control rate close to 90% [1]. Incidence of pulmonary toxicity, usually defined as symptomatic radiation pneumonitis (RP), is reported to be less than 10% [2] due to focused radiation to a small target which spares large volume of healthy lung [3]. However, several non-dosimetric factors reportedly increase or decrease the RP risk, such as central tumor location [4], baseline interstitial pneumonitis [5] and chronic obstructive pulmonary disease (COPD) [6]. Ignoring these factors could underestimate RP risk for certain patients. Thus, there is a clinical need to augment dosimetric RP models with patient-specific clinical and biological risk modifiers towards more patient-specific predictions.

We propose Bayesian network (BN) as a multivariate modeling platform to accommodate such high-dimensional data. BN can be characterized as graphical representation of relationships between input variables called a directed acyclic graph (DAG). Variables in a DAG are connected along the direction of influence. This allows us to study such a radiobiological system as a "whole" whereas conventional multivariate models such as logistic regression are limited to the predictive value of variables in a model [7]. The BN approach has been adopted by a number of outcome studies [8] [9] [10], and specifically for radiation pneumonitis from conventional fractionation [11] where finding a consensus of prediction results from several BN models (ensemble approach) was shown to improve RP prediction. However, the BN approach has not been applied to SBRT cases where dose-volume metrics and biological damage relationships are still not well understood.

The aim of this study is to develop a Bayesian Network RP model for NSCLC SBRT patients. While a primary objective is to assess its predictive potential, we will also address its ability to uncover underlying radiobiological relationships and generate new hypotheses.

2. Materials and Methods

2.1. Patient cohort

Forty three stage I and II NSCLC patients were recruited for this study prospectively from three institutions upon approval of respective ethics review boards: McGill University Health Centre (MUHC), Centre Hospitalier de l'Université de Montréal (CHUM), and Washington University in St. Louis (WashU), 32 patients from MUHC and CHUM formed the training cohort for BN modeling.

11 patients from WashU were reserved for model validation. Every patient met the following eligibility criteria: 1) received SBRT of equal or less than 5 fractions with curative intent, 2) no history of previous lung irradiation, and 3) baseline Karnofsky performance status ≥ 70. Detailed cohort characteristics are summarized in table 1. The patients were treated with radiotherapy (RT) without any adjuvant treatment. Depending on institutions, three different delivery techniques were used: 3-dimensional (3D) conformal radiotherapy, RapidArc™(Varian Medical Systems, Palo Alto, CA) Volumetric Arc Therapy (VMAT), and CyberKnife (Accuray Inc, Sunnyvale, CA). Detailed RT procedures are provided in supplementary tables 1 and 2.

2.2. Data collection

Blood samples from the patients were first acquired on the CT simulation day as a baseline and at 6 weeks post-treatment. Enzyme-linked immunosorbent assay (ELISA) was used for measuring biomarker concentrations in the samples. Incidence rate of symptomatic RP, classified as Common Toxicity Criteria for adverse events (CTCAE) toxicity (version 4) grade 2 or higher, was 13% (4/32) in the training and 9% (1/11) in the validation cohort. Median follow-up was 12 and 34 months for the training and validation cohorts, respectively.

2.3. Candidate variables

Candidate variables for the BN pneumonitis model were chosen from 3 main categories: biological, dosimetric and clinical variables. Candidate biological variables consisted of serum concentration of interleukin(IL)-6, IL-8, angiotensin converting enzyme (ACE), alpha-2-macroglobulin (α2M) , and transforming growth factor (TGF)-β1 and plasma concentration of osteopontin (OPN). As summarized in [12], these biomarkers represent different biological processes involved in pathogenesis of radiation-induced lung injury, such as pro-(IL-6 [13], OPN [14]) and anti-(IL-8 [15]) inflammatory reactions, fibrogenesis (TGFβ [16]), vascular damage (ACE [17]) and modulation of inflammatory reactions (α2M [18]). 12 features in total were extracted (6 biomarkers x 2 time points). The biomarker features at 6-weeks were calculated as percentage difference from respective baseline levels. The following 7 clinical RP risk factors were chosen by literature survey: superoinferior PTV location (PTVCOMSI) [19], age [20], smoking status [21], COPD [6], ACE inhibitor [22], baseline interstitial lung disease [5], and centrally located tumours [4]. Dosimetric factors were derived from planned dose converted to equivalent dose in 2 Gy fraction (EQD2) using an

Table 1: Characteristics of the training and validation cohorts. *Calculated for whole lung subtracted from planning target volume and converted to equivalent dose in 2 Gy fraction (EQD2).

	Patient count (%)	
	Training	Validation
Cohort size	32	11
Tumor stage		
I	32 (100)	9 (81)
II	0 (0)	2 (19)
RP grades		
0	17 (53)	0 (0)
1	11 (34)	10 (91)
2	2 (6)	0 (0)
3	2 (6)	1 (9)
≥ 4	0 (0)	0 (0)
≥ 2	4 (13)	1 (9)
Mean lung dose*		
median	4.9	6.3
range	2.4-10.9	1.2-9.9
RT modality		
3D conformal	19 (59)	11 (100)
VMAT	5 (16)	0 (0)
CyberKnife	8 (25)	0 (0)
RT prescription		
60 Gy in 3 fractions	8 (25)	0 (0)
60 Gy in 5 fractions	5 (16)	1 (9)
50 Gy in 5 fractions	4 (13)	4 (36)
48 Gy in 3 fractions	12 (38)	0 (0)
34 Gy in 1 fractions	3 (9)	0 (0)
54 Gy in 3 fractions	0 (0)	5 (45)
55 Gy in 5 fractions	0 (0)	1 (9)

alpha-beta ratio of 4 Gy for lung [23] and 2 Gy for heart [24]. For lung dose calculation, PTV was subtracted from contoured lung. Mean lung dose (MLD) and various Vx values (lung volume receiving $>$ x Gy) for ipsilateral and whole lung were estimated. Due to high correlation between these parameters [25], exploratory analysis was performed to find the smallest number of features that can capture dose heterogeneity relevant to RP. In this analysis, Vx was computed at various threshold dose x in three different ways: 1) x as an absolute dose or relative to prescription dose, 2) Vx normalized to lung volume or as a absolute volume, and 3) ipsilateral or whole lung. In addition to lung dose, we also considered mean heart dose (MHD) [26], fraction size [27], and PTV volume [28].

2.4. Bayesian Network training

A Bayesian network ensemble model was trained from the candidate variables following the methods developed in [11]. In brief, the training was done in 4 steps:

1. Data discretization: Every continuous variable was discretized into 2 bins at a boundary that maximizes mutual information with respect to RP, as shown in supplementary table 3.
2. Feature selection with the Koller-Sahami (KS) filter: The number of candidate variables were reduced to the smallest subset that maximized explanatory power measured by cross-entropy with respect to RP.
3. DAG training: Posterior distribution of Bayesian network graphs was obtained by Markov-Chain Monte Carlo sampling under causality constraints between variables.
4. Parameter learning: Every variable in a BN is treated as a probabilistic distribution which is conditioned upon its upstream variables ("parents"). BN parameters, referred to as conditional probability values for every pair of a node and its parents, were learned from data using the expectation-maximization algorithm.

2.5. BN model testing

The trained BN ensemble model derived probability of RP using known input variables. Classification of RP events was made by thresholding the RP probabilities. Classification performance was measured using three receiver operating characteristics (ROC) metrics: area under the curve (AUC), sensitivity, and specificity at the optimal operating threshold maximizing the sum of sensitivity and specificity. Model statistical testing was carried out in two ways: 1) the .632+ bootstrap

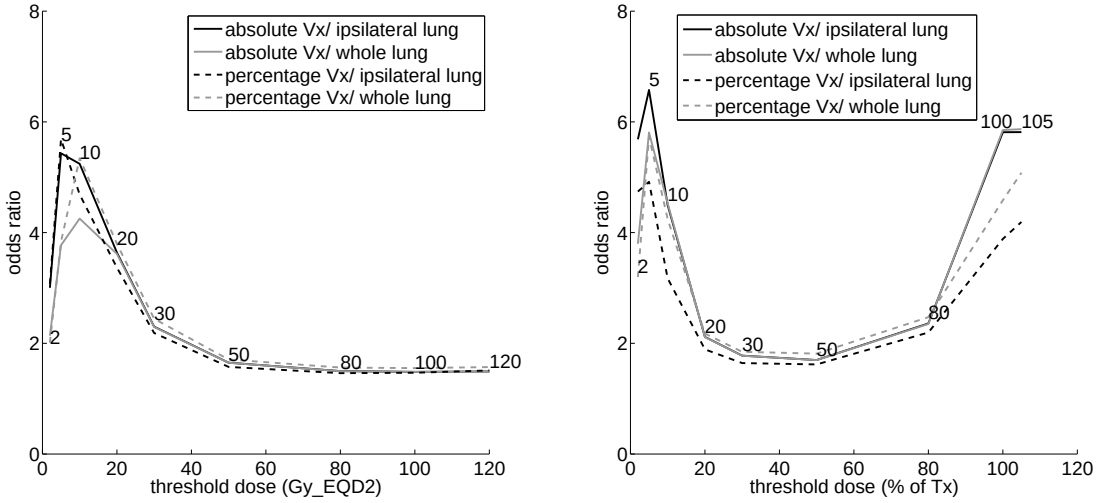

Figure 1: Odds ratios of lung Vx measured at various threshold dose values (x), normalization schemes, and lung volume definition.

method [29]: the training was repeated in 200 replicates which were resampled from the original data with replacement where the instances that were not sampled into the replicates were used for testing. 2) the final model was trained using the entire training set and tested in the validation cohort.

3. Results

3.1. Exploratory analysis of lung DVH parameters

Correlation between lung Vx and RP was examined by the change in odds ratios at various threshold dose (x) (figure 1). When x was used as absolute dose, highest odds ratio (5.685) was marked at 5 Gy for ipsilateral lung. When the percentage of a prescription dose was used as x, increase in correlation was observed in high dose regions beyond 50% of the prescription dose. Guided by this analysis, we chose two Vx parameters that represent low and high dose spillage in this order: percentage of ipsilateral lung volume receiving 5 Gy or more (V5) and absolute lung volume receiving more than 105% of prescription dose (V105%). In a similar fashion, ipsilateral MLD (odds ratio: 2.400) was preferred over MLD for the whole lung (odds ratio: 2.365).

3.2. Variable selection and the Bayesian Network ensemble model

The KS filter reduced the candidate (dosimetric, biological, and clinical) variables from 25 into the following 6 (supplementary table 3): 1) pre-treatment OPN, 2) 6 weeks ACE, 3) pre-treatment TGFβ, 4) ipsilateral V5, 5) V105%, and 6) PTVCOMSI. Inter-relationships between these variables and RP were established in the BN graphs. Bootstrap testing on BN graph learning detected 11 statistically significant links out of possible 19 from an ensemble of 50 graphs where bootstrapped RP prediction performance achieved optimality (figure 3). A mean confidence level of the significant links was 0.57, while the upper bound of random variation was estimated to be 0.29 [30].

3.3. Prediction performance of the BN model

When bootstrap validation was used, RP prediction improved upon increasing number of graphs in an ensemble (figure 3). Optimal performance was achieved at an ensemble size of 50 where AUC, sensitivity and specificity were 0.99, 1, and 0.98, respectively. At the optimal classification threshold, sensitivity was consistently higher than specificity. In external validation, AUC was the highest (0.8) at ensemble sizes 5-30. The BN model was subsequently tested using only the information available at baseline i.e. without ACE at 6 weeks. As a result, AUC and sensitivity decreased significantly at all ensemble sizes. In the validation cohort, however, slightly better performance was observed with only baseline information.

4. Discussion

Events of RP from lung SBRT are rare and identifying the susceptible patients before radiotherapy remains a difficult task, with conflicting results between studies. This study intended to objectively select and combine RP risk factors into a Bayesian Network and test its predictive power. Two factors account for good bootstrap performance of the resulting model in the training cohort. First, the main driving force was strong individual predictive power of the key variables in the model. Univariate AUC values of ACE at 6 weeks, V5, and V105%, 3 variables connected to RP with high confidence, were respectively 0.94, 0.85 and 0.96 in the training cohort. Another factor was the use of an ensemble instead of a single model, which improved performance both in training and validation cohorts. Predictive benefit of an ensemble approach was already shown by other outcome studies [11] [31].

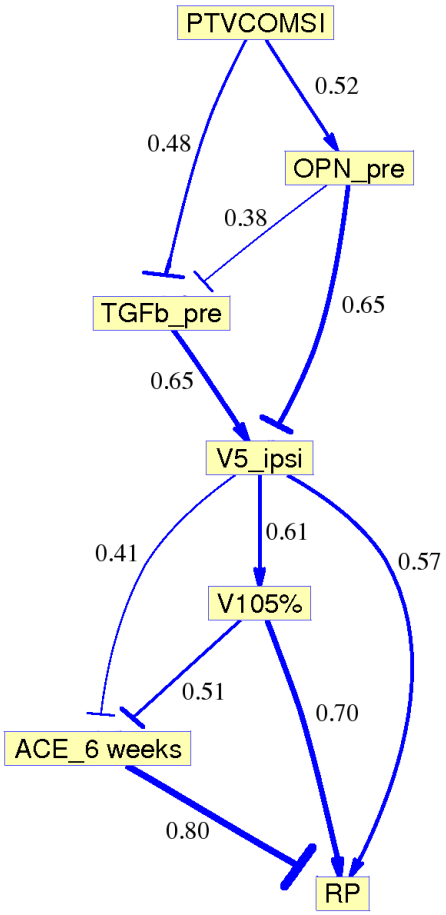

Figure 2: Variables connected by significant associations detected in an ensemble of 50 graphs. Edge thickness was drawn proportionally to bootstrap estimated confidence level. Arrow-headed and bar-headed edges are assigned to positive and negative correlations, respectively. ipsi: ipsilateral lung, _pre: baseline biomarker levels

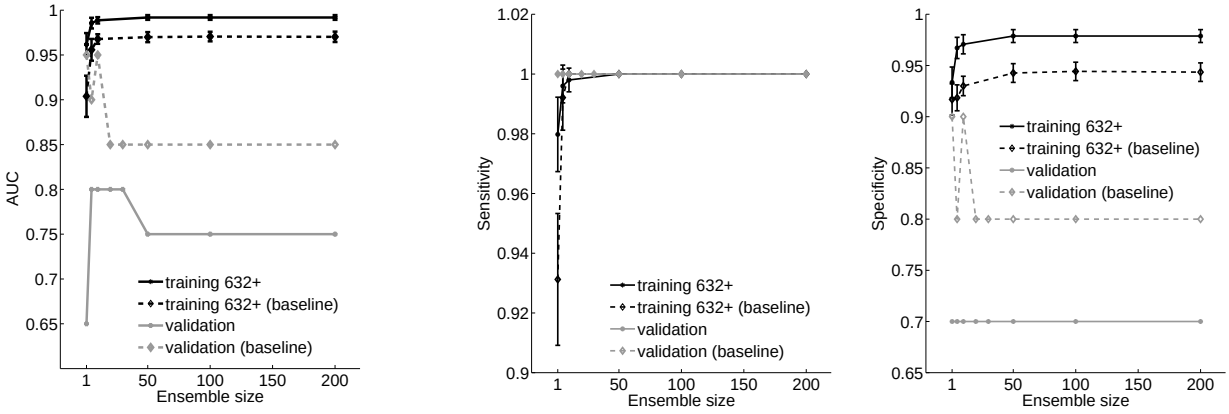

Figure 3: Classification performance of the Bayesian Network model in two cohorts with varying ensemble size. Error bars: bootstrap-estimated 95% confidence intervals.

Amongst the biomarkers we studied, we found lower concentration of ACE at 6 weeks was strongly associated with RP events. This result is in line with investigation by Zhao et al. [16] who reported lower ACE level at baseline and mid-treatment for patients with RP grade ≥ 2. In the Bayesian network ensemble the ACE was connected to dosimetric variables with high confidence. Causality of this relationship could be inferred from the knowledge that the main secretion site of ACE happens in lung epithelium and external stress to pulmonary vasculature such as ionizing radiation or Bleomycin exposure decreases serum ACE [17]. The use of ACE inhibitors at baseline, however, was not a significant predictor of RP ($p = 0.64$) indicating that direct measurement of ACE expression could be a more sensitive test to predict RP.

Choice of 6 weeks as a time point to gauge post-treatment biomarker response was adequate to predict late toxicity before it happened, as the earliest occurrence of RP was 94 days post-RT. However, such information would not be available for the treatment planning stage inn such a case. We tested this scenario by attempting prediction with masked ACE values where the BN model can cope with missing information by marginalizing probability distribution over unknown variables. The role of ACE was not clearly shown in our external validation cohort where the absence of such information did not reduce performance. Although these issues need to be confirmed in larger trial, our model predictions with post-RT variables may aid in monitoring high-risk patients or in prescribing anti-inflammatory medications.

We also observed that the size of high dose spillage, represented by lung volume outside PTV receiving dose $> 105\%$, was predictive of RP in univariate analysis and also one of the key variables in the BN model. This "high dose effect" on RP has been previously reported by a number of studies [19] [32]. Our results on exploratory analysis on Vx point out that both low-dose (V5) and high dose components might be relevant to RP. Previous lung SBRT protocols including RTOG 0236 and 0813 stipulate this volume as one of the quality assurance metrics to be regulated, setting its upper limit on 15% of the PTV volume. Further studies may be needed to clarify the effects of smaller volume of high dose irradiation to lung leading to RP onset.

The main limitation of the current study is the low number of toxicity events in the evaluated cohorts, which led to relatively low specificity of the optimized model. Nevertheless, our computational approach reduced the data dimensionality and identified key variables that may mitigate the impact of a low event rate on fitting. Also, the links that we discovered in the BN graphs represent influential effects among variables that is not necessarily causal always. However, such knowledge may help provide new insights and guide generating new data-driven hypotheses.

5. Conclusion

We developed a Bayesian Network ensemble for modeling radiation pneumonitis after lung SBRT. The process of building the model and the resulting model structure identified potential key players in predicting RP in NSCLC SBRT patients such as high dose spillage to the lung and changes in post-treatment ACE expression levels. This probabilistic model can potentially provide new insights into RP onset and help guide designing new studies as the interest of expanding SBRT to higher risk populations continues to grow.

Conflict of Interest

None.

Acknowledgement

We thank Dr. Jean-François Carrièr and Dr. Robert Doucet for contributing to the clinical data. The computational work was enabled in part by computer resources provided by WestGrid (www.westgrid.ca). This research was partly funded by the Canadian Institute of Health Research

(CIHR) grant MOP-114910. S.L is supported by NSERC CREATE Medical Physics Research Training Network grant 432290.

References

References

[1] R. Timmerman, R. Paulus, J. Galvin, et al., Stereotactic body radiation therapy for inoperable early stage lung cancer, JAMA 303 (11) (2010) 1070–1076.

[2] A. Chi, Z. Liao, N. P. Nguyen, J. Xu, B. Stea, R. Komaki, Systemic review of the patterns of failure following stereotactic body radiation therapy in early-stage non-small-cell lung cancer: Clinical implications, Radiotherapy and Oncology 94 (1) (2010) 1 – 11.

[3] H. Yamashita, W. Takahashi, A. Haga, K. Nakagawa, Radiation pneumonitis after stereotactic radiation therapy for lung cancer, World J Radiol 6 (9) (2014) 708–15.

[4] R. Timmerman, R. McGarry, C. Yiannoutsos, et al., Excessive toxicity when treating central tumors in a phase ii study of stereotactic body radiation therapy for medically inoperable early-stage lung cancer, J Clin Oncol 24 (30) (2006) 4833–9.

[5] H. Yamashita, S. Kobayashi-Shibata, A. Terahara, et al., Prescreening based on the presence of ct-scan abnormalities and biomarkers (KL-6 and SP-D) may reduce severe radiation pneumonitis after stereotactic radiotherapy, Radiat Oncol 5 (2010) 32.

[6] A. Takeda, E. Kunieda, T. Ohashi, et al., Severe copd is correlated with mild radiation pneumonitis following stereotactic body radiotherapy, Chest 141 (4) (2012) 858–66.

[7] I. E. Naqa, J. Bradley, A. I. Blanco, et al., Multivariable modeling of radiotherapy outcomes, including dose–volume and clinical factors, International Journal of Radiation Oncology*Biology*Physics 64 (4) (2006) 1275 – 1286.

[8] W. P. Smith, J. Doctor, J. Meyer, I. J. Kalet, M. H. Phillips, A decision aid for intensity-modulated radiation-therapy plan selection in prostate cancer based on a prognostic bayesian network and a markov model, Artif. Intell. Med. 46 (2) (2009) 119–130.

[9] K. Jayasurya, G. Fung, S. Yu, et al., Comparison of bayesian network and support vector machine models for two-year survival prediction in lung cancer patients treated with radiotherapy, Medical Physics 37 (4) (2010) 1401–1407.

[10] J. H. Oh, J. Craft, R. A. Lozi, et al., A bayesian network approach for modeling local failure in lung cancer, Physics in Medicine and Biology 56 (6) (2011) 1635.

[11] S. Lee, N. Ybarra, K. Jeyaseelan, et al., Bayesian network ensemble as a multivariate strategy to predict radiation pneumonitis risk, Medical Physics 42 (5) (2015) 2421–2430.

[12] K. Fleckenstein, B. Gauter-Fleckenstein, I. L. Jackson, Z. Rabbani, M. Anscher, Z. Vujaskovic, Using biological markers to predict risk of radiation injury, Seminars in Radiation Oncology 17 (2) (2007) 89 – 98.

[13] Y. Chen, P. Rubin, J. Williams, E. Hernady, T. Smudzin, P. Okunieff, Circulating IL-6 as a predictor of radiation pneumonitis, International Journal of Radiation Oncology*Biology*Physics 49 (3) (2001) 641 – 648.

[14] Anthony O'Regan, The role of osteopontin in lung disease, Cytokine and Growth Factor Reviews 14 (6) (2003) 479 – 488.

[15] J. P. Hart, G. Broadwater, Z. Rabbani, et al., Cytokine profiling for prediction of symptomatic radiation-induced lung injury, International Journal of Radiation Oncology*Biology*Physics 63 (5) (2005) 1448 – 1454.

[16] L. Zhao, L. Wang, W. Ji, et al., Association between plasma angiotensin-converting enzyme level and radiation pneumonitis, Cytokine 37 (1) (2007) 71 – 75.

[17] B. Bénéteau-Burnat, B. Baudin, Angiotensin-converting enzyme: Clinical applications and laboratory investigations on serum and other biological fluids, Critical Reviews in Clinical Laboratory Sciences 28 (5-6) (1991) 337–356.

[18] J. H. Oh, J. M. Craft, R. Townsend, J. O. Deasy, J. D. Bradley, I. El Naqa, A bioinformatics approach for biomarker identification in radiation-induced lung inflammation from limited proteomics data, Journal of Proteome Research 10 (3) (2011) 1406–1415.

[19] A. J. Hope, P. E. Lindsay, I. E. Naqa, et al., Modeling radiation pneumonitis risk with clinical, dosimetric, and spatial parameters, International Journal of Radiation Oncology*Biology*Physics 65 (1) (2006) 112 – 124.

[20] I. R. Vogelius, S. M. Bentzen, A literature-based meta-analysis of clinical risk factors for development of radiation induced pneumonitis, Acta Oncologica 51 (8) (2012) 975–983.

[21] H. Jin, S. L. Tucker, H. H. Liu, et al., Dose-volume thresholds and smoking status for the risk of treatment-related pneumonitis in inoperable non-small cell lung cancer treated with definitive radiotherapy, Radiotherapy and Oncology 91 (3) (2009) 427 – 432.

[22] S. Bracci, M. Valeriani, L. Agolli, V. D. Sanctis, R. M. Enrici, M. F. Osti, Renin-angiotensin system inhibitors might help to reduce the development of symptomatic radiation pneumonitis after stereotactic body radiotherapy for lung cancer, Clinical Lung Cancer.

[23] J. B. S. M. Bentzen, J. Z. Skoczylas, Quantitative clinical radiobiology of early and late lung reactions, International Journal of Radiation Biology 76 (4) (2000) 453–462.

[24] S. Schultz-Hector, K.-R. Trott, Radiation-induced cardiovascular diseases: Is the epidemiologic evidence compatible with the radiobiologic data?, International Journal of Radiation Oncology*Biology*Physics 67 (1) (2007) 10 – 18.

[25] L. B. Marks, S. M. Bentzen, J. O. Deasy, et al., Radiation dose-volume effects in the lung, International Journal of Radiation Oncology*Biology*Physics 76 (3, Supplement 1) (2010) S70 – S76.

[26] E. X. Huang, A. J. Hope, P. E. Lindsay, et al., Heart irradiation as a risk factor for radiation pneumonitis, Acta Oncologica 50 (1) (2011) 51–60.

[27] M. Roach, D. R. Gandara, H. S. Yuo, et al., Radiation pneumonitis following combined modality therapy for lung cancer: analysis of prognostic factors., Journal of Clinical Oncology 13 (10) (1995) 2606–12.

[28] Z. Allibhai, M. Taremi, A. Bezjak, et al., The impact of tumor size on outcomes after stereotactic body radiation therapy for medically inoperable early-stage non-small cell lung cancer, International Journal of Radiation Oncology*Biology*Physics 87 (5) (2013) 1064 – 1070.

[29] B. Efron, R. Tibshirani, Improvements on cross-validation: The 632+ bootstrap method, Journal of the American Statistical Association 92 (438) (1997) 548–560.

[30] M. Scutari, On the prior and posterior distributions used in graphical modelling, Bayesian Analysis 8 (3) (2013) 505–532.

[31] S. K. Das, S. Chen, J. O. Deasy, S. Zhou, F.-F. Yin, L. B. Marks, Combining multiple models to generate consensus: Application to radiation-induced pneumonitis prediction, Medical Physics 35 (11) (2008) 5098–5109.

[32] H. Yamashita, K. Nakagawa, N. Nakamura, et al., Exceptionally high incidence of symptomatic grade 2-5 radiation pneumonitis after stereotactic radiation therapy for lung tumors, Radiation Oncology 2 (1) (2007) 21.

[33] R. D. Timmerman, An overview of hypofractionation and introduction to this issue of seminars in radiation oncology, Seminars in Radiation Oncology 18 (4) (2008) 215 – 222.

[34] Y. Benjamini, Y. Hochberg, Controlling the false discovery rate: A practical and powerful approach to multiple testing, Journal of the Royal Statistical Society. Series B (Methodological) 57 (1) (1995) 289–300.

Supplemental Materials for: Modeling of Radiation Pneumonitis after Lung Stereotactic Body Radiotherapy: A Bayesian Network Approach

Table 1: Detailed radiotherapy procedures used for the training cohort. GTV: gross tumour volume, ITV: internal target volume, IGTV: internal gross tumour volume, PTV: planning target volume, Tx: prescription dose, 4DCT: 4-dimensional computed tomography, IGRT: image-guided radiotherapy, fx: fraction, MU: monitoring unit.

Institution	MUHC	CHUM	
Technique	3D-CRT	VMAT	CyberKnife
Dose prescription	Dose normalized to 100 % at Tx, 95% of PTV receives Tx or higher (D95% $\geq$ Tx)	Dose normalized to 100 % at Tx which covers 95% or more of the PTV	
Dose planning procedure/ calculation algorithm	Forward planning using Eclipse (Varian, USA)/ superposition-convolution algorithm with heterogeneity correction	Inverse planning with RapidArc (Varian, USA)/ superposition-convolution algorithm with heterogeneity correction	Inverse planning with Multiplan (Accuray, USA) / Monte Carlo calculation
Beam type	6 MV photon	6 MV photon	6 MV photon
Target volume definition	ITV: drawn from 4DCT using maximum intensity projection PTV: ITV + 5 mm margin	IGTV: drawn on extreme phases of 4DCT to represent its full extent PTV: IGTV + 5 mm margin	GTV: drawn on breath hold, corrected if needed for deformation/rotation using extreme phases PTV: GTV + 5 mm margin
Dose fractionation	50 Gy in 5 fx: tumor at central location and/or close to critical organs (chest wall/large vessels/spinal cord) 34 Gy in 1 fx: otherwise, upon patients' request for shorter treatment 48 Gy in 3 fx: otherwise	50 Gy in 5 fx: tumour at central location 60 Gy in 5 fx: peripheral tumour close to OARs 60 Gy in 3 fx: otherwise	
Dose constraints to OARs	50 Gy in 5 fx: RTOG 0915 48 Gy in 3 fx: RTOG 0915 34 Gy in 1 fx: RTOG 0813	Timmerman et al. [S33]	
Immobilization	BodyFix (Elekta Oncology, Norcross, GA)	BodyFix (Elekta Oncology)	Vac-Lok (Civco Medical Solutions, Orange City, IA)
IGRT	CBCT at every fraction	Pre- and mid-treatment CBCT at every fraction	Real-time target tracking
Plan verification	Independent MU check	Independent MU check, daily dynalog verification	Independent MU check

Table 2: Detailed radiotherapy procedures used for the validation cohort.

Institution	WashU
Technique	3D-CRT
Dose prescription	Dose generally prescribed to 80% isodose line (range 60-90%) and covers >95% of PTV
Dose planning procedure/ calculation algorithm	Forward planning with 7-11 non-coplanar beams using Pinnacle (Philips, Netherlands)/ superposition-convolution algorithm with heterogeneity corrections
Beam type	6 MV photons
Target volume definition	ITV: drawn from 4DCT using maximum intensity projection PTV: ITV + 5 mm margin
Dose fractionation	50-60 Gy in 5 fx: central location or close to critical organs 54 Gy in 3 fx: all others
Dose constraints to OARs	50-60 Gy in 5 fx: RTOG 0813 54 Gy in 3 fx: RTOG 0618
Immobilization	Abdominal compression (CDR systems, Canada)
IGRT	CBCT at every fraction with KV fluoroscopy
Plan verification	Independent MU check

Table 3: Odds ratios of candidate variables, bin boundary used for discretization, and frequency of selection obtained by bootstrapping the KS variable filtering. P-values were adjusted for multiple comparison using a method by Benjamini and Hochberg [S34]. *variables selected for the BN modeling stage. † taken as a percentage change from baseline.

	Odds ratio (p-value)	Bin boundary	Selection frequency
Biological variables			
OPN (baseline)*	0.887 (0.886)	54.2 ng/ml	0.394
OPN (6 weeks†)	1.150 (0.886)	80.9 %	0.133
IL8 (baseline)	2.862 (0.210)	31.0 pg/ml	0.228
IL8 (6 weeks)	0.404 (0.637)	-60.4 %	0.264
ACE (baseline)	1.999 (0.529)	141.1 ng/ml	0.308
ACE (6 weeks)*	0.002 (0.010)	-15.8 %	0.782
IL6 (baseline)	0.070 (0.657)	7.0 pg/ml	0.2
IL6 (6 weeks)	1.106 (0.886)	-7.0 (%)	0.058
a2M (baseline)	0.553 (0.638)	5.3 mg/ml	0.328
a2M (6 weeks)	0.848 (0.886)	-7.6 %	0.142
TGFb (baseline)*	1.866 (0.540)	42.2 ng/ml	0.504
TGFb (6 weeks)	0.493 (0.610)	1.4 %	0.053
Dosimetric variables			
MLD (ipsilateral)	2.400 (0.391)	13.8 Gy	0.107
V5 (ipsilateral)*	5.685 (0.060)	42.4 %	0.454
V105%*	5.848 (0.023)	1.4 cc	0.668
Fraction size	0.752 (0.886)	20 Gy per fraction	0.142
PTV volume	1.932 (0.518)	20.5 cc	0.064
MHD	1.945 (0.529)	9.0 Gy	0.153
Clinical variables			
PTVCOMSI*	0.379 (0.391)	0.5	0.448
Age	1.172 (0.886)	69	0.121
Smoking	1.077 (0.945)		0.146
IP	1.300 (0.768)		0.061
Central tumour	1.800 (0.854)		0.068
COPD	0.750 (0.886)		0.120
ACE inhibitor	0.800 (0.638)		0.054